Suppression of neutron superfluidity in neutron star crusts

Nicolas Chamel

Institute of Astronomy and Astrophysics
Université Libre de Bruxelles, Belgium

IJC Lab, Orsay, 21 Mars 2023

Neutron stars: laboratories for dense matter

Formed in gravitational core-collapse supernova explosions, neutron stars are the **most compact stars** in the Universe.

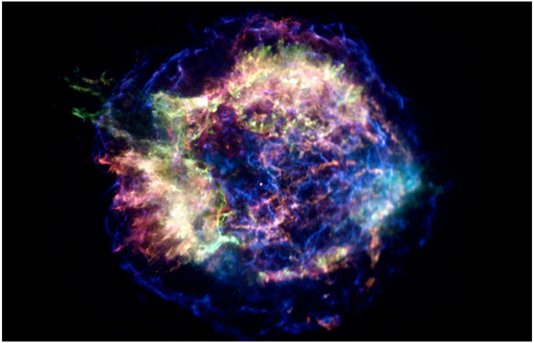

Nuclear physics:

$M \sim 1 - 2M_\odot$
$R \sim 10$ km
$\Rightarrow \rho \sim 10^{15}$ g cm^{-3}

Energy scale: MeV

"cold" $\lesssim 10^{10}$ K $\lesssim$ "hot"

Neutron stars are initially very hot ($\sim 10^{12}$ K) but cool down to $\sim 10^9$ K within days by releasing neutrinos.

Their dense matter is thus expected to undergo various phase transitions, as observed in terrestrial materials at low-temperatures.

Superstars

The huge gravity of neutron stars produces the highest-T_c and largest superfluids and superconductors known in the Universe!

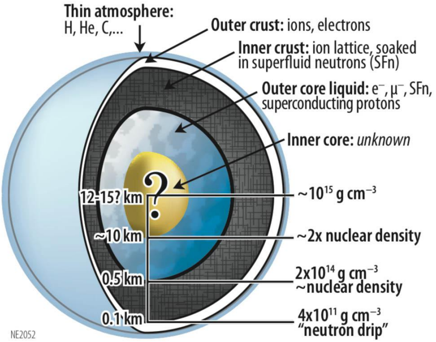

Neutron stars	$\sim 10^{10}$ **K**
$\vdots$	$\vdots$
CH_8S	288 K
Cuprates	1 – 130 K
Electrons in ordinary metals	1 – 25 K
Helium-4	2.17 K
Helium-3	2.491×10^{-3} K
Bosonic condensates	$\sim 10^{-6}$ K
Fermionic condensates	$\sim 10^{-8}$ K

Predicted long ago, these quantum phases may be probed through astrophysical observations.

Pulsar frequency glitches and superfluidity

Pulsars are spinning very rapidly with **extremely stable periods** $\dot{P} \gtrsim 10^{-21}$, outperforming the best atomic clocks.
Milner et al., Phys. Rev. Lett. 123, 173201 (2019)

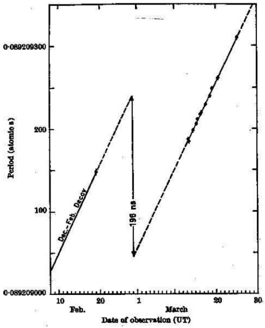

Still, some pulsars have been found to **suddenly spin up** (in less than a minute).

670 glitches have been detected in 208 pulsars.
`http://www.jb.man.ac.uk/pulsar/glitches.html`

Recent review: *Zhou et al.,Universe 8(12), 641(2022)*

The first glitch was detected in Vela in 1969.
Radhakrishnan&Manchester, Nature 222, 228 (1969)
Reichley&Downs, ibid. 229

Pulsar glitches provide strong evidence for neutron superfluidity in neutron star-crusts.

Time-dependent Hartree-Fock-Bogoliubov theory

The dynamics of nuclear superfluids ($q = n, p$) is described by the **time-dependent Hartree-Fock-Bogoliubov equations**:

$$\begin{pmatrix} h_q(\boldsymbol{r},t) - \lambda_q & \Delta_q(\boldsymbol{r},t) \\ \Delta_q(\boldsymbol{r},t)^* & -h_q(\boldsymbol{r},t)^* + \lambda_q \end{pmatrix} \begin{pmatrix} \psi_1^{(q)}(\boldsymbol{r},t) \\ \psi_2^{(q)}(\boldsymbol{r},t) \end{pmatrix} = \mathrm{i}\hbar \frac{\partial}{\partial t} \begin{pmatrix} \psi_1^{(q)}(\boldsymbol{r},t) \\ \psi_2^{(q)}(\boldsymbol{r},t) \end{pmatrix}$$

$$h_q(\boldsymbol{r},t) \equiv -\boldsymbol{\nabla} \cdot \frac{\hbar^2}{2m_q^{\oplus}(\boldsymbol{r},t)} \boldsymbol{\nabla} + U_q(\boldsymbol{r},t) - \frac{\mathrm{i}}{2} \left\{ \boldsymbol{I_q}(\boldsymbol{r},t), \boldsymbol{\nabla} \right\} + \dots$$

$$\frac{\hbar^2}{2m_q^{\oplus}(\boldsymbol{r},t)} = \frac{\delta E}{\delta \tau_q(\boldsymbol{r},t)}, \quad U_q(\boldsymbol{r},t) = \frac{\delta E}{\delta n_q(\boldsymbol{r},t)}, \quad \boldsymbol{I_q}(\boldsymbol{r},t) = \frac{\delta E}{\delta \boldsymbol{j_q}(\boldsymbol{r},t)}$$

$$\Delta_q(\boldsymbol{r},t) = 2 \frac{\delta E}{\delta \widetilde{n_q}(\boldsymbol{r},t)^*} = |\Delta_q(\boldsymbol{r},t)| e^{\mathrm{i}\phi_q(\boldsymbol{r},t)}$$

with mean fields defined via the **particle and pair density matrices** (thermal averages) expressible in terms of $\psi_1^{(q)}(\boldsymbol{r},t)$ and $\psi_2^{(q)}(\boldsymbol{r},t)$

$$n_q(\boldsymbol{r},\sigma;\boldsymbol{r'},\sigma';t) = < c_q(\boldsymbol{r'},\sigma';t)^\dagger c_q(\boldsymbol{r},\sigma;t) >$$

$$\widetilde{n}_q(\boldsymbol{r},\sigma;\boldsymbol{r'},\sigma';t) = -\sigma' < c_q(\boldsymbol{r'},-\sigma';t) c_q(\boldsymbol{r},\sigma;t) >$$

Superfluid velocities are not true velocities

The **superfluid velocity** defined through the phase of the pairing field

$$\boldsymbol{V_q}(\boldsymbol{r},t) = \frac{\hbar}{2m_q}\nabla\phi_q(\boldsymbol{r},t)$$

is neither equal to $\hbar\boldsymbol{j_q}/\rho_q$ where $\boldsymbol{j_q}$ is the **momentum density**

$$\boldsymbol{j_q}(\boldsymbol{r},t) = -\frac{i}{2}\sum_{\sigma=\pm1}\int \mathrm{d}^3\boldsymbol{r'}\,\delta(\boldsymbol{r}-\boldsymbol{r'})(\nabla-\nabla')n_q(\boldsymbol{r},\sigma;\boldsymbol{r'},\sigma;t)$$

nor to the **true velocity**

$$\boldsymbol{v_q}(\boldsymbol{r},t) = \frac{m_q}{m_q^{\oplus}(\boldsymbol{r},t)}\frac{\hbar\boldsymbol{j_q}(\boldsymbol{r},t)}{\rho_q(\boldsymbol{r},t)} + \frac{\boldsymbol{I_q}(\boldsymbol{r},t)}{\hbar}$$

associated with **mass transport**

$$\frac{\partial\rho_q}{\partial t} + \nabla\cdot(\rho_q\boldsymbol{v_q}) = 0$$

Chamel & Allard, PRC100, 065801 (2019); Allard & Chamel, PRC103, 025804 (2021)

Neutron superfluidity in neutron-star crusts

The breaking of translational symmetry leads to the existence of a normal-fluid component even at zero temperature.

In the presence of a **superflow** with velocity $\boldsymbol{V_n}$, the average neutron mass current in the rest frame of the neutron-star crust is

$$\bar{\rho}_n^i \equiv \frac{1}{V}\int \mathrm{d}^3 r\, \rho_n(\boldsymbol{r},t) v_n^i(\boldsymbol{r},t) = \sum_j \rho_s^{ij} \bar{V}_{n\,j}$$

Treating the crust as a polycrystal $\bar{\boldsymbol{\rho}}_{\boldsymbol{n}} = \rho_s \bar{\boldsymbol{V}}_{\boldsymbol{n}} = \rho_n \dfrac{m_n}{m_n^\star} \bar{\boldsymbol{V}}_{\boldsymbol{n}}$.

The superfluid density $\rho_s < \rho_n$ ($m_n^\star > m_n$) is a **current-current response function**.

ρ_s"is a derived concept and is not the density of anything".

Feynman, Statistical Mechanics: A Set of Lectures.

Review: *Chamel, J. Low Temp. Phys. 189, 328 (2017)*

Neutron superfluidity in neutron-star crusts

In the absence of superflow $V_n = 0$:

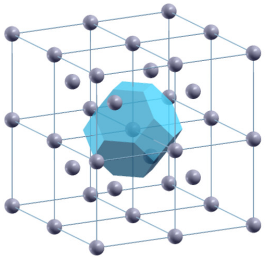

Floquet-Bloch theorem:

$\psi_{1\alpha\boldsymbol{k}}(\boldsymbol{r}+\boldsymbol{\ell}) = e^{\mathrm{i}\,\boldsymbol{k}\cdot\boldsymbol{\ell}}\psi_{1\alpha\boldsymbol{k}}(\boldsymbol{r})$

$\psi_{2\alpha\boldsymbol{k}}(\boldsymbol{r}+\boldsymbol{\ell}) = e^{\mathrm{i}\,\boldsymbol{k}\cdot\boldsymbol{\ell}}\psi_{2\alpha\boldsymbol{k}}(\boldsymbol{r})$

for any lattice vector $\boldsymbol{\ell}$.

band index α: rotational symmetry
wave vector $\boldsymbol{k}$: translational symmetry.

The HFB equations need to be solved only in the **Wigner Seitz cell** with $\boldsymbol{k}$ restricted to the first Brillouin zone.

3D HFB computations remain expensive:

- Lattice spacing can be large ~ 100 fm
- Huge number of neutrons in the Wigner-Seitz cell ($\sim 10^2 - 10^3$)

From HFB to multi-band BCS theory

Due to **proximity effects**, $\Delta(\boldsymbol{r})$ varies smoothly: $\psi_{1\alpha\boldsymbol{k}} \approx \mathcal{U}_{\alpha\boldsymbol{k}}\varphi_{\alpha\boldsymbol{k}}$, $\psi_{2\alpha\boldsymbol{k}} \approx \mathcal{V}_{\alpha\boldsymbol{k}}\varphi_{\alpha\boldsymbol{k}}$, where $h(\boldsymbol{r})\varphi_{\alpha\boldsymbol{k}}(\boldsymbol{r}) = \varepsilon_{\alpha\boldsymbol{k}}\varphi_{\alpha\boldsymbol{k}}(\boldsymbol{r})$.

The HFB equations reduce to the **multiband BCS gap equations**:

$$\Delta_{\alpha\boldsymbol{k}} = -\frac{1}{2}\sum_{\beta}\int \frac{\mathrm{d}^3\boldsymbol{k'}}{(2\pi)^3}\,\bar{v}^{\rm pair}_{\alpha\boldsymbol{k}\alpha-\boldsymbol{k}\beta\boldsymbol{k'}\beta-\boldsymbol{k'}}\,\frac{\Delta_{\beta\boldsymbol{k'}}}{E_{\beta\boldsymbol{k'}}}\tanh\frac{E_{\beta\boldsymbol{k'}}}{2k_{\rm B}T}$$

$$\bar{v}^{\rm pair}_{\alpha\boldsymbol{k}\beta\boldsymbol{k'}} = \int \mathrm{d}^3r\, v^{\pi}[n_n(\boldsymbol{r}), n_p(\boldsymbol{r})]\,|\varphi_{\alpha\boldsymbol{k}}(\boldsymbol{r})|^2|\varphi_{\beta\boldsymbol{k'}}(\boldsymbol{r})|^2$$

where $E_{\alpha\boldsymbol{k}} = \sqrt{(\varepsilon_{\alpha\boldsymbol{k}}-\lambda)^2 + \Delta_{\alpha\boldsymbol{k}}^2}$ and $v^{\pi}[n_n(\boldsymbol{r}), n_p(\boldsymbol{r})]$ is an effective pairing interaction. The HFB solutions read

$$\mathcal{U}_{\alpha\boldsymbol{k}} = \frac{1}{\sqrt{2}}\sqrt{1+\frac{\varepsilon_{\alpha\boldsymbol{k}}-\lambda}{E_{\alpha\boldsymbol{k}}}}, \quad \mathcal{V}_{\alpha\boldsymbol{k}} = -\frac{1}{\sqrt{2}}\sqrt{1-\frac{\varepsilon_{\alpha\boldsymbol{k}}-\lambda}{E_{\alpha\boldsymbol{k}}}}$$

Chamel et al., Phys.Rev.C81,045804 (2010)

Multi-band BCS superconductors

Multi-band superconductors were first studied in 1959 but clear evidence were found only in 2001 with the discovery of MgB_2.

Electrons in different bands feel different pairing interactions leading to different pairing gaps:

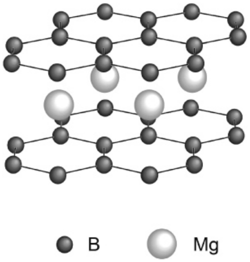

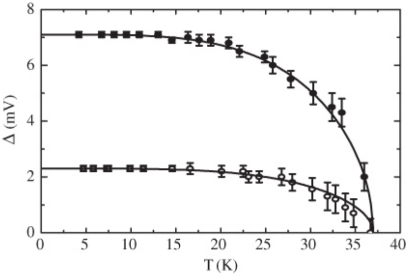

X. X. Xi, Rep. Prog. Phys.71, 116501 (2008)

In the crust of a neutron star, the number of bands involved is $\sim 10^2 - 10^3$ due to strong attractive nuclear pairing interactions!

Multi-band BCS neutron superfluid

Wigner-Seitz cell with $Z = 40$, $N = 1220$ (body-centered cubic lattice)

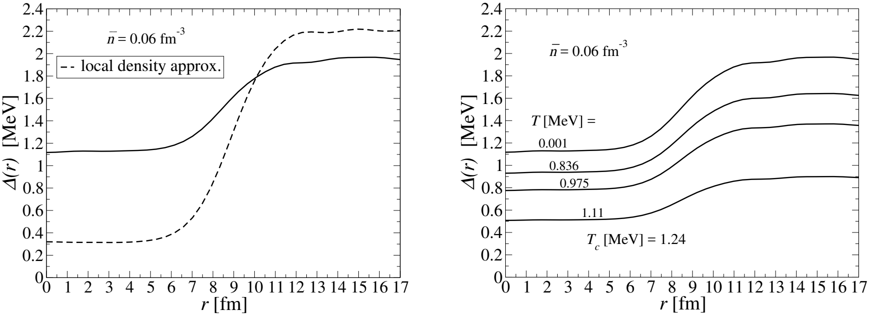

Chamel et al., Phys.Rev.C81,045804 (2010)

- Both bound and unbound neutrons contribute to superfluidity
- Superfluidity permeates clusters (loosely bound Cooper pairs)
- The superfluid becomes homogeneous as T approaches T_c
- Nuclear clusters lower the gap by $\sim 10-20\%$

Neutron superfluid fraction

In the limit of small currents, the neutron superfluid density is given by

$$\rho_s = \frac{m_n^2}{24\pi^3\hbar^2} \sum_\alpha \int \mathrm{d}^3\boldsymbol{k} |\mathcal{V}_{\alpha\boldsymbol{k}}|^2 \sum_i \frac{\partial^2 \varepsilon_{\alpha\boldsymbol{k}}}{\partial k_i \partial k_i} \,.$$

In the **weak coupling** limit $\Delta_{\alpha\boldsymbol{k}}/\varepsilon_{\mathrm{F}} \to 0$

$$\rho_s \approx \frac{m_n^2}{12\pi^3\hbar^2} \sum_\alpha \int \mathrm{d}^3\boldsymbol{k}\, \delta(\varepsilon_{\alpha\boldsymbol{k}} - \lambda) |\boldsymbol{\nabla}_{\boldsymbol{k}} \varepsilon_{\alpha\boldsymbol{k}}|^2$$

ρ_s is fully determined by the shape of the Fermi surface
independently of pairing

$$\rho_s = \frac{m_n^2}{12\pi^3\hbar^2} \sum_\alpha \int_{\mathrm{F}} |\boldsymbol{\nabla}_{\boldsymbol{k}} \varepsilon_{\alpha\boldsymbol{k}}| \mathrm{d}\mathcal{S}^{(\alpha)}$$

Carter,Chamel,Haensel,Nucl.Phys.A748,675 (2005); Nucl.Phys.A759,441(2005)

Neutron superfluid fraction in shallow region

Neutron band structure (s.p. energy in MeV vs $\boldsymbol{k}$) in a body-centered cubic (bcc) lattice at $\bar{n} = 0.0003$ fm^{-3} ($Z = 50, A = 200$):

First Brillouin zone:

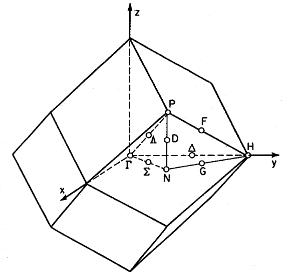

Chamel,Phys.Rev.C85,035801(2012)

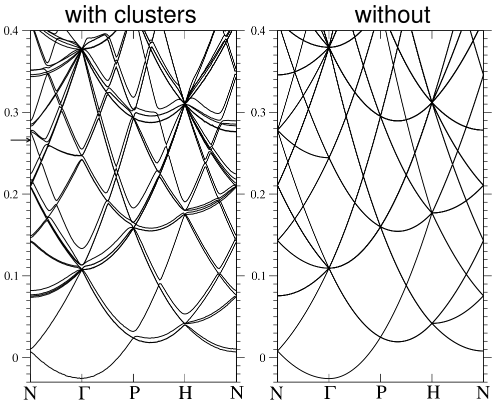

The spectrum is similar that of free neutrons: $\rho_s/\rho_n = 83\%$.

Neutron superfluid fraction in deep region

Neutron band structure (s.p. energy in MeV vs $\boldsymbol{k}$) in a body-centered cubic (bcc) lattice at $\bar{n} = 0.03$ fm^{-3} ($Z = 40, A = 1590$):

First Brillouin zone:

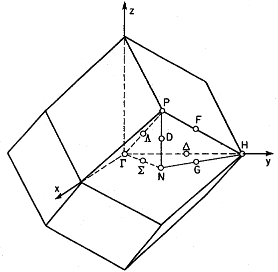

Chamel,Phys.Rev.C85,035801(2012)

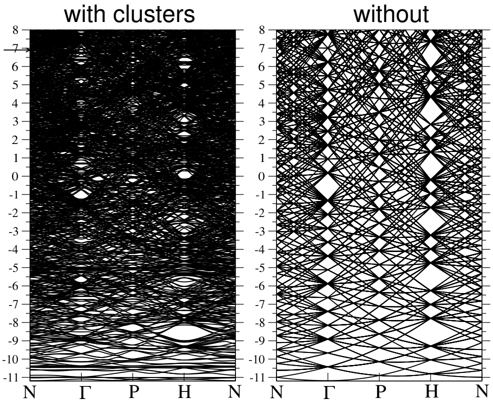

The spectrum is very different: $\rho_s/\rho_n = 7\%$. Neutron superfluidity is almost entirely suppressed!

Band structure and Fermi surface

Bragg scattering leads to strong distortions of the Fermi surface.

Avoided band crossings where

$$|\nabla_{\boldsymbol{k}} \varepsilon_{\alpha \boldsymbol{k}}| \sim 0$$

translate into necks and holes reducing the Fermi surface area.

Both effects suppress the superfluid density

$$\rho_s = \frac{m_n^2}{12\pi^3\hbar^2} \sum_\alpha \int_{\mathrm{F}} |\nabla_{\boldsymbol{k}} \varepsilon_{\alpha \boldsymbol{k}}| \mathrm{d}\mathcal{S}^{(\alpha)}$$

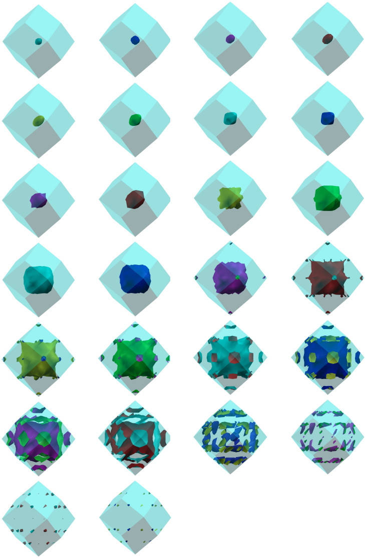

Picture made with XCrySDen

Hydrodynamical approach

The neutron flow was studied in the **strong coupling limit** adopting a purely **classical hydrodynamical** treatment.

- Superfluid velocity: $\boldsymbol{V_n} = \frac{\hbar}{2m_n}\nabla\Phi$
- Incompressible superfluid flow: $\nabla \cdot \boldsymbol{V_n} = 0$
- Spherical clusters (obstacles) with sharp surfaces.

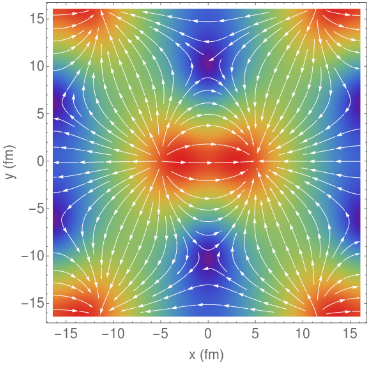

Classical potential flow $\Delta\Phi = 0$

The neutron mass current is

$$\boldsymbol{\rho_n} \equiv \rho_n \boldsymbol{v_n} = \frac{1}{\mathcal{V}_{\rm cell}} \int_{\rm cell} n_n(\boldsymbol{r})\nabla\Phi(\boldsymbol{r})$$
$$= \rho_s \boldsymbol{V_n}$$

Martin&Urban,Phys.Rev.C94, 065801(2016)

Classical potential flow past obstacles

Permeability of the clusters:
$\delta = 0$ no superfluidity,
$\delta = 1$ superfluidity everywhere.
Martin&Urban,Phys.Rev.C94,065801(2016)

Added perturbations from different clusters are negligible.
Epstein, ApJ333, 880 (1988)

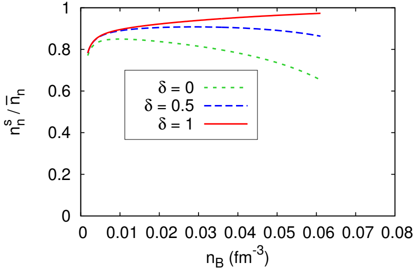

The potential flow past a single cluster can be solved analytically:

$$\frac{\rho_s}{\rho_n} = 1 + 3\frac{\mathcal{V}_{\rm cl}}{\mathcal{V}_{\rm cell}}\frac{\delta-\gamma}{\delta+2\gamma} \qquad \gamma = \frac{\rho_n^{\rm free}}{\rho_n^{\rm cluster}}$$

Magierski&Bulgac,Act.Phys.Pol.B35,1203(2004); Magierski, IJMPE13, 371(2004)
Sedrakian, Astrophys.Spa.Sci.236, 267(1996); Epstein, ApJ333, 880 (1988)

The superflow is found to be only **weakly perturbed** by clusters.
However, the strong coupling regime may not be reached.

Suppression of band structure effects by pairing?

By solving the HFB equations in the limit of small currents, Watanabe&Pethick (2017) found that

- **superfluidity is more strongly suppressed** than predicted by hydrodynamics
- **but much less than band calculations without pairing**: $\rho_s/\rho_n \sim 60 - 70\%$ instead of $\sim 7\%$ for $\bar{n} = 0.03$ fm^{-3}.

Watanabe&Pethick,PRL119,062701(2017)

But many **simplying approximations** were made:

- 3D body-centered cubic lattice replaced by a **1D lattice**
- pairing potential $\Delta(\boldsymbol{r})$ not solved self-consistently but fixed
- numerical extraction of ρ_s from second derivatives of the energy with respect to superfluid velocity V_n
- **unrealistically weak potential**

Suppression of band structure effects by pairing?

Band-structure effects arise from the HF equation:

$$h(\boldsymbol{r})\varphi_{\alpha\boldsymbol{k}}(\boldsymbol{r}) = -\nabla \cdot B(\boldsymbol{r})\nabla\varphi_{\alpha\boldsymbol{k}}(\boldsymbol{r}) + U(\boldsymbol{r})\varphi_{\alpha\boldsymbol{k}}(\boldsymbol{r}) = \varepsilon_{\alpha\boldsymbol{k}}\varphi_{\alpha\boldsymbol{k}}(\boldsymbol{r})$$

Chamel (2012): $h(\boldsymbol{r})$ from extended Thomas Fermi approach
Watanabe&Pethick (2017): $B(r) = \hbar^2/(2m_n)$ and $U(r) = 2V_K \cos(Kr)$

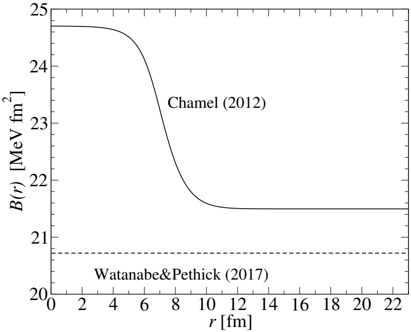

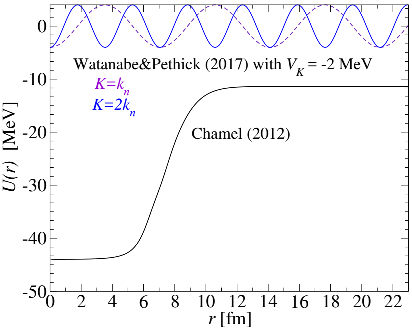

Role of pairing further examined

Full **3D band-structure** calculations (body-centered cubic lattice) using **realistic Hamiltonian** (same as in 2012)

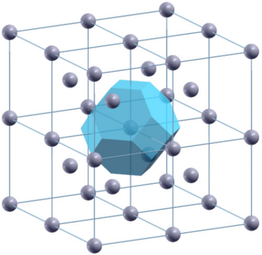

Floquet-Bloch boundary conditions:

$\psi_{1\alpha\boldsymbol{k}}(\boldsymbol{r}+\boldsymbol{\ell}) = e^{\mathrm{i}\,\boldsymbol{k}\cdot\boldsymbol{\ell}}\psi_{1\alpha\boldsymbol{k}}(\boldsymbol{r})$

$\psi_{2\alpha\boldsymbol{k}}(\boldsymbol{r}+\boldsymbol{\ell}) = e^{\mathrm{i}\,\boldsymbol{k}\cdot\boldsymbol{\ell}}\psi_{2\alpha\boldsymbol{k}}(\boldsymbol{r})$

for any lattice vector $\boldsymbol{\ell}$.

- pairing included in the **BCS approximation**
- superfluid density from **analytical** formula

$$\rho_s = \frac{m_n^2}{24\pi^3\hbar^2}\sum_\alpha \int |\nabla_{\boldsymbol{k}}\varepsilon_{\alpha\boldsymbol{k}}|^2 \frac{\Delta^3}{\sqrt{(\varepsilon_{\alpha\boldsymbol{k}}-\lambda)^2+\Delta^2}^3}\mathrm{d}^3k$$

- **realistic gaps** Δ from extended BHF calculations

  Cao, Lombardo,Schuck, Phys.Rev. C 74, 064301 (2006)

Role of pairing further examined

Numerical results obtained using a parallelized code based on plane waves using FFT and condensed-matter physics techniques.

Δ (MeV)	$\Delta/\varepsilon_{\rm F}$	ρ_s/ρ_n (%)
1.59	0.0869	7.50
1.11	0.0604	7.50
0.770	0.0420	7.51
0.535	0.0292	7.54
0.372	0.0203	7.60
0. 259	0.0141	7.66
0.180	0.00981	7.71
0.125	0.00682	7.76
0.0869	0.00474	7.80
0.0604	0.00330	7.82
0.0420	0.00229	7.84

$\bar{n} = 0.03$ fm^{-3}
bcc lattice spacing 47.3 fm
1550 neutrons in the Wigner-Seitz cell

$25 \times 25 \times 25$ points ($\delta r \sim 0.95$ fm)
$\sim$ 1300 bands (half without pairing)

integrations with 1360 special $\boldsymbol{k}$ points
(65 280 $\boldsymbol{k}$ points in the first Brillouin zone)

$\sim 10^6$ s.p. wavefunctions

Including pairing is computationally very costly, but results are essentially the same as those obtained without.

Superfluidity in nuclear lasagna

Self-consistent HF calculations (no pairing):

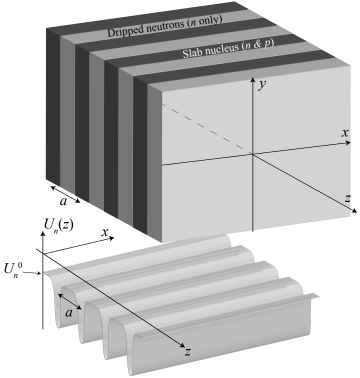

alternative definitions of
$m_n^\star/m_n = \rho_n/\rho_s$ due to ambiguity in ρ_n

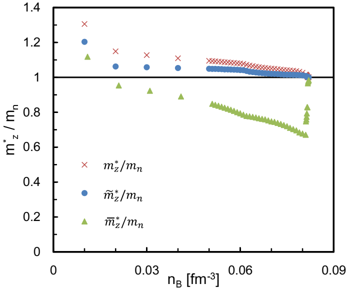

Kashiwaba & Nakatsukasa, PRC 100,035804(2019)

Superfluid density ρ_s consistent with previous calculations from
Carter, Chamel, Haensel, Nucl. Phys. A748, 675 (2005).

Superfluidity in nuclear lasagna

Self-consistent **time-dependent** HF calculations (no pairing):

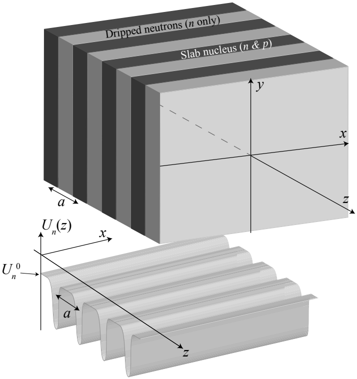

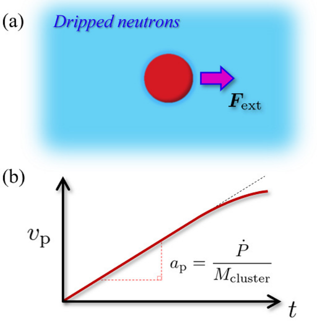

Sekizawa et al. , PRC 105,045807(2022)

Dynamic treatment consistent with static band calculations.

Superfluidity in nuclear lasagna

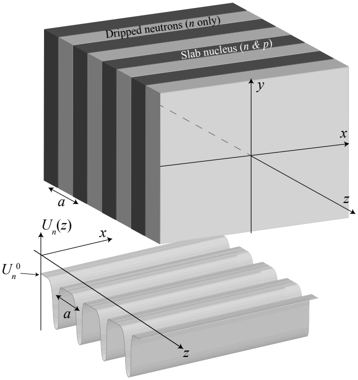

Sekizawa et al. , PRC 105,045807(2022)

Counter flow of free neutrons ?

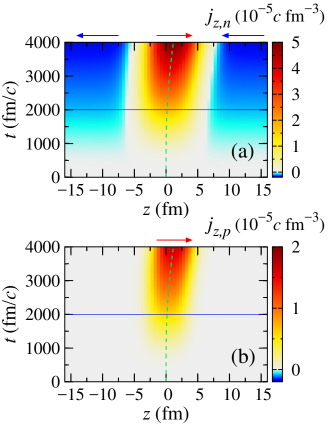

But $j_{z,n}(z)$ negligible outside the slab "nucleus" and parallel to $j_{z,p}(z)$ inside: neutrons are still entrained by the crust

Pairing vs Bragg scattering

Toy model: 3 bands in 1D lattice with potential $U(z) = 2V\cos(Kz)$

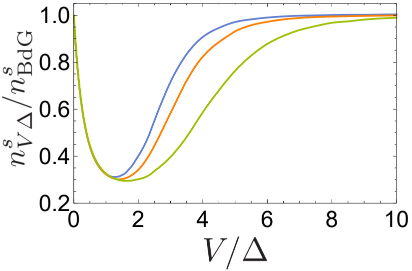

Superfluid density:

$n^s_{V\Delta}$ (BCS) vs n^s_{BdG} (HFB)

Fixed pairing gap Δ:

$\Delta/\varepsilon_F = 0.01$ (green), 0.05 (orange), 0.1 (blue)

Minami&Watanabe, Phys. Rev. Res. 4, 033141 (2022)

For realistic model at $\bar{n} = 0.03\ \mathrm{fm}^{-3}$, $V/\Delta \approx 10$ and $\Delta/\varepsilon_F \approx 0.09$.

The neutron superfluid density in neutron-star crusts can be accurately estimated using the BCS approximation.

Role of disorder

Superfluidity appears to be very sensitive to the structure of the crust.

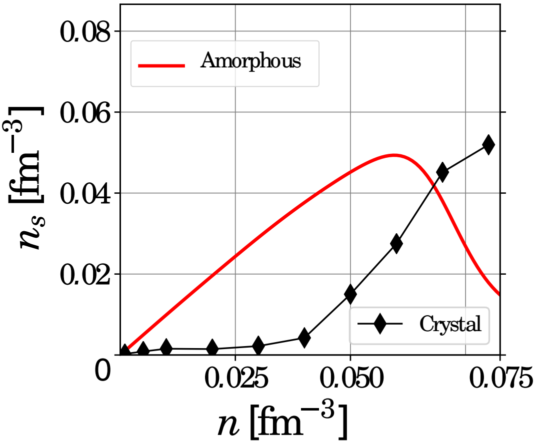

Sauls,Chamel,Alpar, arXiv:2001.09959

Conclusions

Superfluid neutrons in neutron-star crusts do not flow freely due to the breaking of translational symmetry.

- **Full 3D band-structure calculations with BCS pairing** confirm the suppression of superfluidity due to Bragg scattering.
- **Superfluidity is also suppressed in amorphous crusts** but mainly in densest layers.
- **The superfluid dynamics has astrophysical implications** (e.g. pulsar glitches).

Open questions:

- Role of composition (catalyzed vs accreted crusts)?
- Superfluidity in nuclear pastas?
- Collective excitations?
- Breaking of superfluidity? Critical currents?